Wireless Networks
https://doi.org/10.1007/s11276-021-02658-3

A novel microstrip array circular polarized antenna based on t-type power divider

Lulu Bei[1] · Lu Zhang[2] · Kai Huang[3]

Abstract
In underground wireless communication in the coal mines, it is necessary for antenna to have good penetration and multi-path resistance to coal dust and water mist. The circular polarization antenna has two orthogonal fields, horizontal and vertical, and the circular polarization antenna has better penetration in coal seam water mist than the linear polarization antenna under the same power. The circular polarization is divided into left rotation polarization and right rotation polarization, and the antenna can only receive signals in the same polarization direction. In the process of underground propagation, the signal is easily reflected by obstacles, changes the polarization direction, and is not received by the original polarization direction antenna. In the underground environment of the coal mine, it can be used as an effective solution to resist multi-path. An array circular polarization antenna based on T power divider and uniform rotary the feed network is proposed in this paper. The circuit structure of 16-unit micro-strip array circular polarization antenna is introduced. The structure and working principle of feed network and antenna are analyzed. Finally, simulation and experiment show that the antenna has the advantages of high front-to-back ratio, is suitable for long-distance and high orientation reading and writing applications, and is very suitable for RFID long-distance reading and writing applications in coal mine long and narrow environment. It has good application prospects and economic benefits.

Keywords Communication systems · T-type power divider · Circular polarization · Micro-band antennas · Feed networks

1 Introduction

The underground roadway in the coal mine is a kind of communication space that is limited, heterogeneous, non-uniform and time-varying. During the underground propagation of electromagnetic wave signal, it is affected by the equipment such as roadway, coal wall surface, production and safety, which will make the electromagnetic waveform reflection, scattering and diffraction, which will cause multi-path effect and lead to the fading of the signal. In addition, in the process of underground mining, the irregularity of moving targets such as personnel and equipment and coal seam water mist will also increase the randomness and volatility of signal multi-path reflection and attenuation [1, 2]. For the purpose of improving the quality of underground communication, scholars have constantly tried to study the citation of new technologies. Some key technologies have made breakthrough progress in the application and improvement of advanced wireless communication technologies such as smart antenna, MIMO (Multi-Input Multi-Output), cognitive radio and so on [3–5].

With the rapid development of modern wireless communication technology, wireless communication has

✉ Lu Zhang
yulu7517@126.com

Lulu Bei
beilulu66@126.com

Kai Huang
hk-830110@163.com

[1] Jiangsu Province Key Laboratory of Intelligent Industry Control Technology, Xuzhou University of Technology, Xuzhou 221018, Jiangsu, China

[2] School of Mathematics and Statistics, Xuzhou University of Technology, Xuzhou 221018, Jiangsu, China

[3] JiangSu XCMG Information Technology Co., LTD, Xuzhou 221008, China

Published online: 25 June 2021

played an increasingly important role in people's production and life. RF front-end and antenna, as an indispensable part of the communication system, play a key role in the quality of the whole communication system. The RF front-end is mainly composed of microwave passive components such as filters, power splitters, directional couplers, phase shifters and microwave active components such as impedance converters, amplifiers, mixers. The antenna is the key component of signal receiving and transmitting in the wireless communication system. The performance of its feed network directly affects the quality of signal receiving and transmitting. So the feed network applied to the circularly polarized antenna has a good theoretical significance and research value in the field of RF microwave communication.

Wilkinson power divider was first proposed by Ernest J. Wilkinson in a document in 1960. Based on the principle of quarter wavelength impedance conversion, this power divider realizes the matching of any port and the isolation between ports. The disadvantage is that the isolation resistance is located between each output port, which makes it difficult to add a convenient Load radiator, so it can not be used on high-power occasions [6]. To this end, Ulrich H. Gysel proposed an improved Wilkinson power divider, namely Gysel power divider, in 1975. The power divider successfully designs an eight-way combiner with 20% working bandwidth by grounding the isolation resistance. Because of the resistance grounding, it effectively conducts heat and is suitable for high-power occasions. However, no matter Wilkinson power divider or Gysel power divider, due to the use of isolation resistor, it has the disadvantage that it cannot be arbitrarily extended to any path in the plane [7]. Therefore, a Bagley polygon power divider is proposed. Because the isolation between output ports is not considered, only the matching of input ports and the transmission characteristics of the circuit are considered, the circuit structure can be extended to any odd number of paths Therefore, a lot of research has been done[8, 9]. In addition, as the feed network of micro-strip antenna, power divider plays an important role in the design of antenna [10–15]. Next, the power divider theory is applied to the antenna feed network to improve the performance of the antenna. In this paper, a new design method of T-type power divider feed network is proposed, and its simulation and test are carried out.

A read–write antenna is used as a device at the front end of a RFID system. It plays a key role in the performance of the whole system. As RFID technology continues to be used in coal mines, higher requirements for the performance index of the RFID antenna. In a practical application scenario, A low—cost RFID tag usually uses a linear polarization antenna, and its position and position are arbitrary [12, 16–19]. In order to suppress antenna polarization mismatch during reading and writing, RFID reading and writing antennas generally use circular polarization to improve the communication reliability between readers and labels [20–24]. Besides, every country in the world has different bands for RFID systems, Such as 840.5 ∼ 844.5 MHz and 920.5 ∼ 924.5 MHz in China, 866 ∼ 869 MHz in Europe, 902 ∼ 928 MHz in the Americas, 920 ∼ 925 MHz in Singapore and 952 ∼ 955 MHz in Japan. From this point of view, the operating frequency bands of UHF RFID systems used in various countries range from 840 ∼ 960 MHz, and its relative bandwidth is 13.3. If the frequency band of the read–write antenna can cover that frequency range, which will be very beneficial to the low cost design and implementation of the RFID system [25–27]. Besides, In the underground long and narrow tunnel communication space, 2.45 GHz frequency band RFID system requires that the read and write antenna can accurately read and write the specific area range at a distance ahead. This requires a read–write antenna with a large gain and a narrow beam width. There must also be a high ratio [28, 29].

The existing down-hole antenna technology is difficult to meet the needs of its application environment. According to the down-hole demand, a high-performance microstrip array antenna with the high front-back ratio for long-distance RFID reading and writing applications in 2.45 GHz frequency band is studied. Firstly, the antenna design theory and design method are given, then the antenna model is established by HFSS electromagnetic simulation software. Finally, the antenna object is made and the performance test is completed to verify the antenna.

2 T-type junction function feeder network

2.1 Structure and working principle of feed network

The T-type Power Divider proposed in this section, shown in Fig. 1(a). The input port is the standard 50Ω, and the output port is 100Ω. Based on this Power Divider and micro-band delay line shifter, a four-point power feed network is formed. Figure 1 (b) is a T-type Power Divider based feed network with the same structure for the internal and external branch, but the four output ports of the two feed networks have different characteristic impedances.The characteristic impedance of the internal feed network output port is the standard 50Ω, and the characteristic of the external feed network output port is the input impedance of the rectangular radiation patch of 130Ω. The micro-strip with an electrical length of 180° and 90°, respectively, and a micro-strip with a characteristic impedance of Z_1 is a

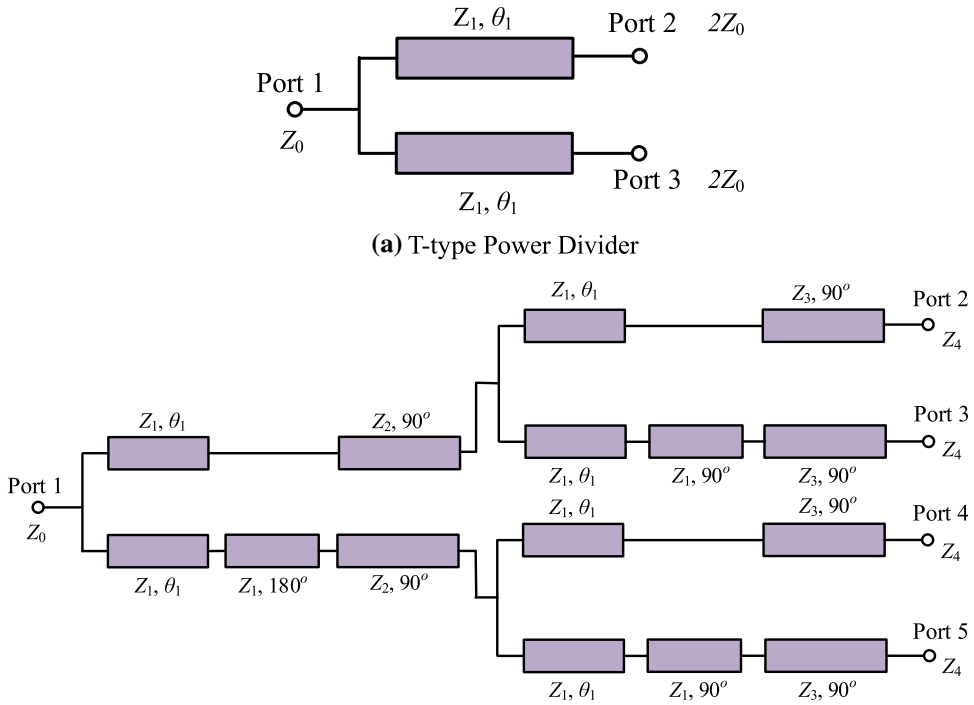

Fig. 1 T-type power divider and its power-divider feed network **a** T-type Power Divider **b** The echo loss of the input port and the insertion loss of the circuit

delay line for both feed networks, with an electrical length of 90°. The micro-strip line with feature impedances *of* Z_2 and Z_3 acts as an impedance converter.

The working principle of the antenna internal power distribution network is analyzed (the working principle of the external power distribution network is the same): the input signal feeds from the input port. The first through the first stage of the machine and 180° delay line shifter, so that the input signal is divided into two signals with equal amplitude and opposite phase. Then the impedance is transformed to the standard 50Ω via a quarter wavelength impedance converter. The two inverted signals are passed through the second stage of the machine and the 90° delay line shifter, respectively. The above two signals are further assigned to two orthogonal signals with an equal phase difference of 90 ^{o}. Finally, the impedance is transformed again to the output port, i.e. 50Ω, through a quarter-wavelength impedance converter. It can be seen that at the center frequency after the input signal passes through the power division phase-shifting feed network, four signals with equal amplitude and phase lag of 90 ^{o} can be obtained at the output port. It is worth noting that the T-type power divider has no isolation resistance, so the matching and isolation of the output port are not considered.

2.2 Simulation and testing

Based on the theory of odd and even mode analysis and two-stage feed network analysis, the expression of the circuit electrical parameters of the internal power division feed network can be obtained: $Z_0 = 50\Omega$, $Z_1 = 100\Omega$, $\theta_1 = 100°$, $Z_2 = 71\Omega$, $Z_3 = 71\Omega$, $Z_4 = 50\Omega$. The expression of the circuit electrical parameters of the external power division feeding network is $Z_0 = 50\Omega$, $Z_1 = 100\Omega$, $\theta_1 = 100°$, $Z_2 = 71\Omega$, $Z_3 = 114\Omega$, $Z_4 = 130\Omega$.

To make it clearer how the function divider to feed network works, Fig. 2 lists the echo loss of the internal function feed network input port, the insertion loss of the circuit, and the phase difference between the output ports.

From Fig. 2(a), it can be seen that at the center frequency 2.45 GHz, Return loss $|S_{11}|$ of the input port is better than 50 dB. The input ports match and the insertion loss is equal $|S_{21}|$,$|S_{31}|$,$|S_{41}|$and$|S_{51}|$. It is proved that the four-way output is an equal energy signal. From Fig. 2(b), it can be seen that the phase difference between output port 3 and output port 2 is -90^o (Phase$|S_{31}|$-$|S_{21}|$= -90°). The phase difference between output port 4 and output port 2 is -180°(Phase $|S_{41}|$-$|S_{21}|$= -180°), and the phase difference between output port 5 and output port 2 is -270°(Phase $|S_{51}|$-$|S_{21}|$= -270°). It is fully proved that the phase difference between the four output ports is 90° in turn, which feeds the circularly polarized antenna. The S-parameters and phase difference of the external power feed network are the same as those of the internal power feed network, which will not be analyzed here. (Fig. 3).

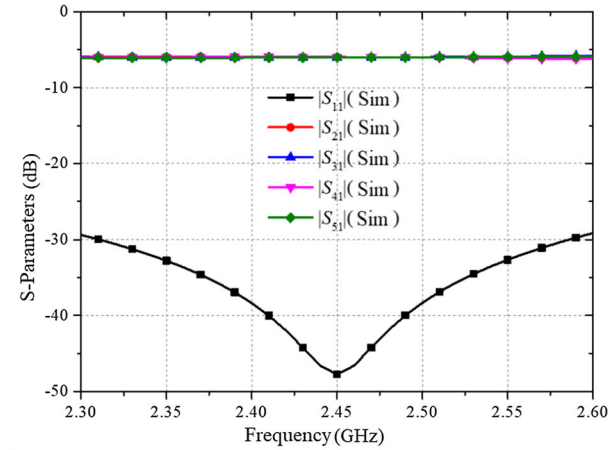

(a) The echo loss of the input port and the insertion loss of the circuit

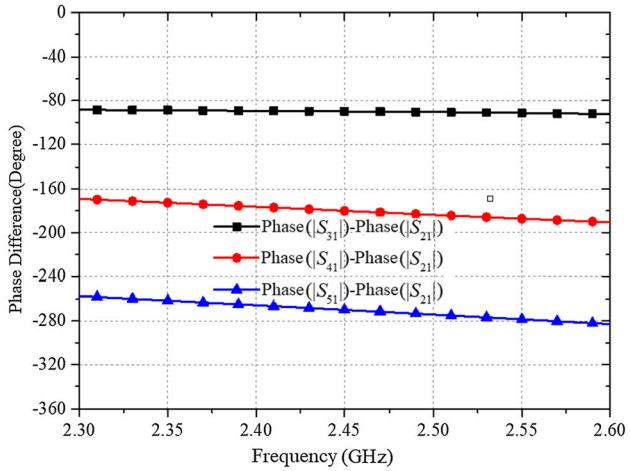

(b) Phase difference between output ports

Fig. 2 Scattering parameters and phase difference of the power divider feed network **a** The echo loss of the input port and the insertion loss of the circuit **b** Phase difference between output ports

3 Array circular polarization antenna

3.1 Structure of the antenna

The circularly polarized array antenna designed in this paper is shown in Fig. 1. It can be seen that the antenna is composed of a two-stage rotary feed network inside and between sub-arrays and 16 square tangent circularly polarized radiation patches. The RF signal is fed into the energy signal through the central feeding point and then fed through the internal one quarter T-type network. The signal is divided into four channels with the same amplitude and a phase lag of 90° in turn. Then each signal is fed into four tangent circular polarized radiation patches through a four-part T- type feed network. It can be seen that the antenna consists of an internal T- type feed network and four external T- type feed networks to form the whole two-stage rotating feed network, and then 16 channels of signals are

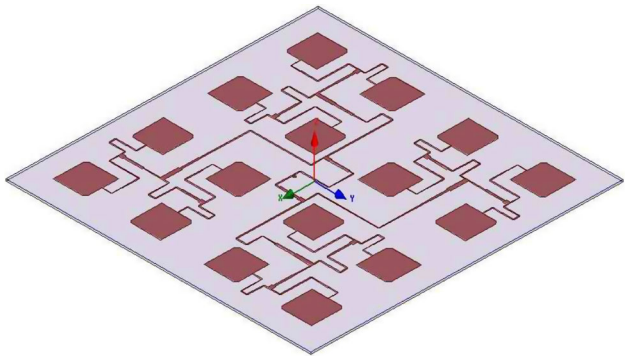

(a) Antenna 3D structural diagram

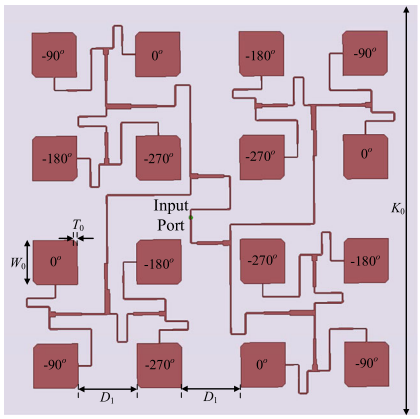

(b) Antenna Top View

Fig. 3 Antenna structure **a** Antenna 3D structural diagram **b** Antenna Top View

fed into 16 square tangent circular polarized radiation patches.

The array antenna is designed with microwave sheet F4B, the thickness of the media substrate is H_0s = 1.5 mm. The dielectric constant is ε_r = 2.65, and the media loss angle tangent value is 0.001. The array unit uses a cut-angle square patch for circular polarization radiation, with the right-angle driven by the cut triangle being T_0 = 2.9 mm, and the patch cell edge length being W_0 = 36 mm. Inside the sub-arrays, the distance between the cell patch is D_1 = 48 mm, between the two sub-arrays, the distance between the adjacent cell patch is D_{1-} = 48 mm mm, and the edge length of the entire array antenna is K_0 = 340 mm.

3.2 Antenna production and experiments

Model and optimize the designed circularly polarized micro-band antenna based on the T-type 16 array using hf-frequency electromagnetic simulation software HFSS, and then use a printed circuit board to make the physical image of the antenna as shown in Fig. 4.

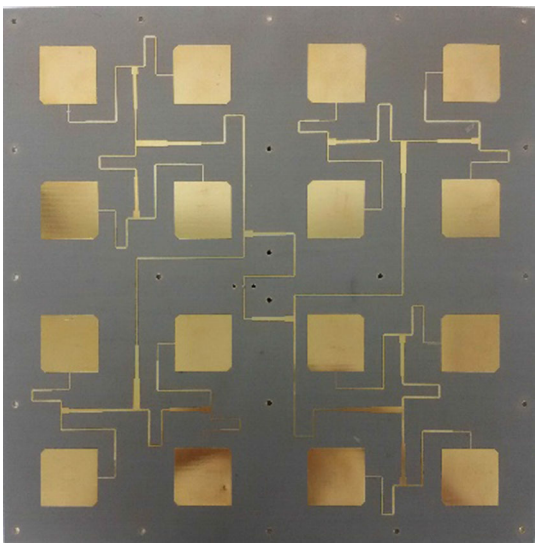

Fig. 4 Fabricated antenna structure

The echo loss and far-field radiation performance of the antenna were tested using Agilent's vector network analyzers E8363B and SATIMO's darkroom test system SG24, respectively, with results shown in Figs. 5 6 and 7. Figure 5 is the echo loss of the antenna, Fig. 6 is the radiation gain in the positive direction of the antenna z axis, and Fig. 7 is the axis ratio of the antenna z axis in the positive direction.

As shown in Fig. 5, the simulation frequency range of antenna return loss $|S_{11}|$ greater than 10 dB is 2.41–2.53 GHz, and the relative bandwidth is 4.9%. The corresponding test frequency range is 2.35–2.55 GHz, and the relative bandwidth is 8.2%. In terms of return loss, the test result is slightly better than the simulation result. It can be seen from Fig. 6 that the simulated peak gain of the antenna is 18.75dBi, the corresponding frequency point is 2.465 GHz, the tested peak gain is 17.60dBi, and the corresponding frequency point is 2.472 GHz. In the frequency band 2.35 ~ 2.55 GHz, the simulated and tested gains are greater than 9.5dbi. It can be seen from Fig. 7 that the simulation-3 dB axial ratio frequency range of the antenna is 2.42 ~ 2.51 GHz, with a relative bandwidth of 3.7%. The corresponding test working frequency range is 2.412 ~ 2.516 GHz, with a relative bandwidth of 4.2%; the above simulation and test results are basically consistent. The antenna is simulated and tested at 2.45 GHz, and the radiation patterns of XoZ and YoZ are obtained, as shown in Fig. 8. The test results show that in the XoZ plane and YoZ plane, the half power beam of the antenna is the same, both are 18°(−10° ~ 8°). It can be seen that the simulation and test results of the antenna are very similar.

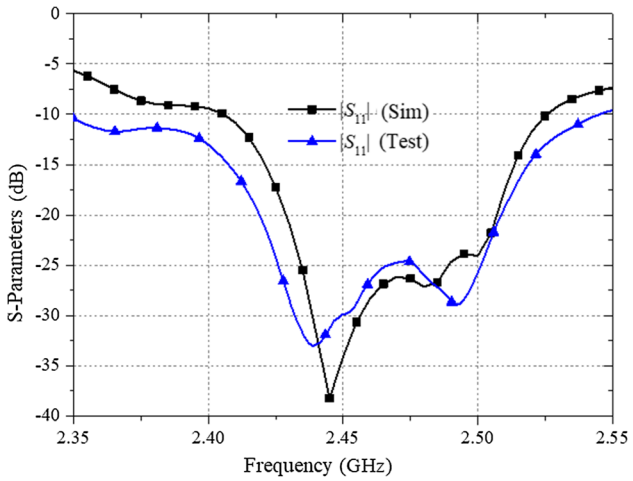

Fig. 5 Simulated and measured return loss

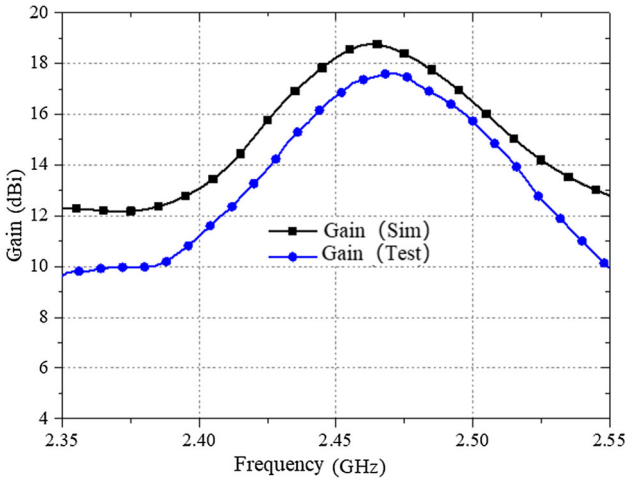

Fig. 6 Simulated and measured antenna gain

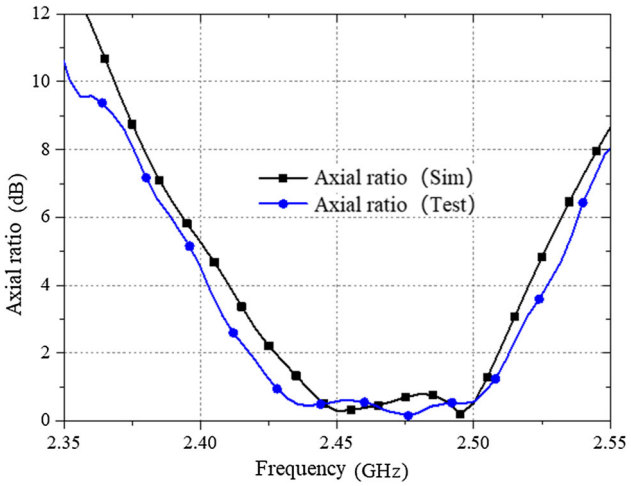

Fig. 7 Simulated and measured axial ratio

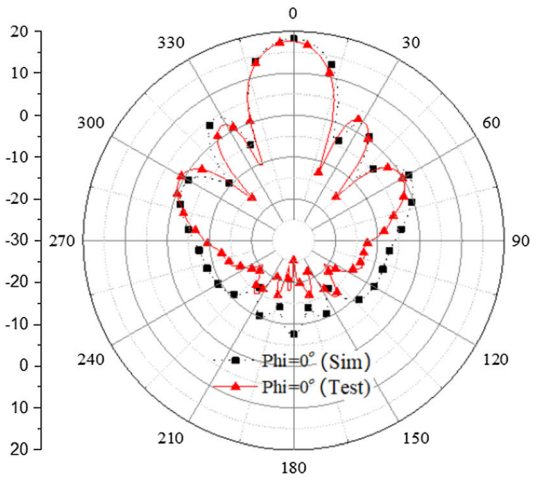

(a) Radiation pattern of XoZ plane at 2.45GHz

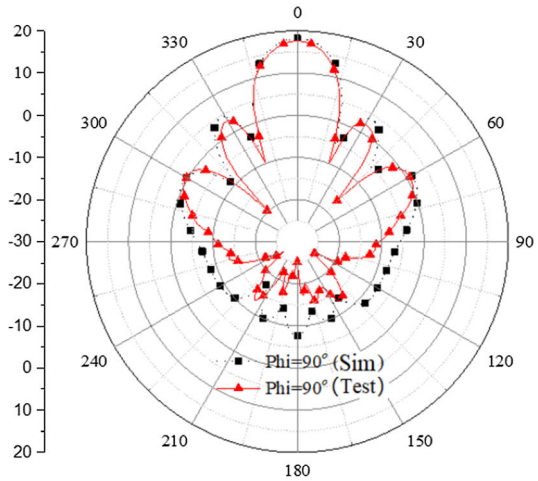

(b) Radiation pattern of YOZ plane at 2.45GHz

Fig. 8 Simulated and measured results of radiation pattern **a** Radiation pattern of XoZ plane at 2.45 GHz **b** Radiation pattern of YOZ plane at 2.45 GHz

4 Conclusions

In summary, the array antenna is mainly based on a two-stage rotating symmetrical structure, square angled circular polarization patch, low-cost low-loss sheet to achieve high-performance RFID reading and writing array antenna. Taking into account the complexity and performance of the design, the feed network adopts the T-type Power Divider, phase shifter and impedance matcher cascade to realize the antenna structure of the feed network and the radiation patch co-face, which not only improves the front-to-front ratio but also helps to reduce the complexity of antenna design and processing and assembly time and cost. The test results show that the echo loss of the antenna is better than 24.5 dB, the axis ratio is better than 0.5 dB, the peak gain is 17.8 dB, and the front and rear ratio is 30 dB. Ideal for the coal mine underground narrow environment RFID long-distance reading and writing applications has good application prospects and economic benefits.

Acknowledgements This work was supported in part by Xu Zhou Science and Technology Plan Project (Grant No. KC19003), the National Natural Science Foundation of China under Grant 62001148 , the Fundamental Research Funds for the Provincial Universities of Zhejiang under Grant GK199900299012-004, and the General Scientific Research Project of Zhejiang Provincial Education Department under Grant Y201942025.

References

1. Huo, Y., Zhao, L., Hu, Q., et al. (2020). Optimal deployment of antenna for field coverage in coal mine tunnels [J]. *IEEE Access, 8*, 51954–51963.
2. Yaqin, Wu, Mengmeng, et al. (2019). A dynamic information platform for underground coal mine safety based on internet of things [J]. *Safety Science, 113*, 9–18.
3. Mohanty, A., Behera, B. R. (2021). Design of a 3-Port Compact MIMO Antenna Based on Characteristics Mode Analysis Approach [J]. Progress In Electromagnetics Research C, 111, 173–189.
4. Soni, U., Kumari,U. (2020). Fault Analysis of Electric Power System using PLC and Wireless Communication System [J]. *International Journal of Engineering and Advanced Technology*, *9*(4), 2249–8958.
5. Khelladi, H., Mograne, M. A. (2019). Optimization of some acoustic parameters intended for the wireless communication in seawater [J]. *Applied Acoustics, 154*(11):59–67.
6. Wilkinson, E. J. (1960). An N-way hybrid power divider [J]. *Microwave Theory and Techniques, IRE Transactions on, 8*(1), 116–118.
7. Gysel, U. H. (1975). A new N-way power divider/combiner suitable for high-power applications [J]. *Microwave Symposium*, 116–118.
8. Elles, D. S., Yoon, Y. K. (2009). Compact dual band three way Bagley polygon power divider using composite right/left handed (CRLH) transmission lines [J]. *Microwave Symposium Digest*, 485–488.
9. Liu, X., Yu, C., Liu, Y., et al. (2010). Design of planar dual-band multi-way power dividers [J]. *Discover the world's research*, 722–725.
10. Moulay, A., & Djerafi, T. (2018). Wilkinson power divider with fixed width substrate-integrated waveguide line and a distributed isolation resistance. *IEEE Microwave Components Letters, 28*(2), 114–116.
11. Sarkar, S., Gupta, B. (2020). A Dual Band Circularly Polarized Antenna with a Dual Band AMC Reflector for RFID Readers [J]. *IEEE Antennas and Wireless Propagation Letters, 19*(5), 796–800.
12. Lee, S. R., Lim, E. H., Bong, F. L., et al. (2020). High-efficient compact folded-patch antenna fed by T-Shaped L-Probe for On-metal UHF RFID tag design[J]. *IEEE Transactions on Antennas and Propagation, 68*(1), 152–160.
13. Kumar, M., Sharma, A., Zuazola, I. (2020). All-in-One UHF RFID Tag Antenna for Retail Garments Using Nonuniform Meandered Lines [J]. *Progress In Electromagnetics Research Letters, 94*(94), 133-139.
14. Aslam, B., Kashif, M., Amin, Y., et al. (2021). Low-profile magnetically coupled dual resonance patch antenna for UHF RFID applications [J]. *AEU - International Journal of Electronics and Communications, 133*, 153672.

15. Salah, H., Robert, J., Ahmed, H. A., et al. (2019). Theoretical Performance Evaluation of UHF-RFID Systems With Multi-Antenna Maximum-Likelihood Decoding [J]. *IEEE Journal of Radio Frequency Identification*, *3*(2), 108–117.
16. Forsythe, P., Fini, A., Yazdi, A. J. (2019). The Value Proposition of RFID Technology in Tall Prefabricated Timber Buildings [J]. *Modular and Offsite Construction (MOC) Summit Proceedings*, 181–188.
17. Alami, A. E., Ghazaoui, Y., Das, S., et al. (2019). Design and Simulation of RFID Array Antenna 2x1 for Detection System of Objects or Living Things in Motion [J]. *Procedia Computer Science*, *151*, 1010–1015.
18. Jebbawi, K., Egels, M., Pannier, P.(2020). A novel compact circularly polarized tag antenna with differential-RFIC for EU UHF RFID applications [J]. *Microwave and Optical Technology Letters, 62*(4), 1621–1627.
19. Bhaskar, S., & Singh, A. K. (2019). Meandered cross-shaped slot circularly polarised antenna for handheld UHF RFID reader – Science Direct [J]. *AEU - International Journal of Electronics and Communications, 100*, 106–113.
20. Chaimool, S., Chung, K. L., Akkaraekthalin, P. (2020). Simultaneous gain and bandwidths enhancement of a single-feed circularly polarized Microstrip patch antenna using a metama-Terial reflective surface [J]. *Progress In Electromagnetics Research B, 22*(22), 23–37.
21. Saeidi-Manesh, H., Zhang, G. (2020). Challenges and Limitations of the Cross-Polarization Suppression in Dual-Polarization Antenna Arrays Using Identical Subarrays [J]. *IEEE Transactions on Antennas and Propagation, 68*(4), 2853–2866.
22. Wang, Z., Dong, Y. (2020). Miniaturized RFID Reader Antennas Based on CRLH Negative Order Resonance [J]. *IEEE Transactions on Antennas and Propagation, 68*(2), 683–696.
23. Nestoros, M., Christou, M. A., Polycarpou, A. C. (2017). Design of wideband, circularly polarized patch antennas for RFID applications in the FCC/ETSI UHF bands [J]. *Progress In Electromagnetics Research C, 78*, 115–127.
24. Yuan, Y., Liang, Y., Yu, J., et al. (2017). Design of a Multipolarized RFID Reader Antenna for UHF Near-Field Applications [J]. *IEEE Transactions on Antennas & Propagation, 65*(7), 3344–3351.
25. HatamiNaseroghadasi, AMohammad. (2018). Split ring resonator metamaterial loads for compact Hepta band printed inverted F antenna with circular polarization [J]. *Microwave and Optical Technology Letters, 60*(10), 2552–2559.
26. Bagheroghli, H., & Zaker, R. (2018). Double triangular monopole-like antenna with reconfigurable single/dual-wideband circular polarization [J]. *International Journal of RF and Microwave Computer-Aided Engineering, 28*(6), e21267.
27. Yuwono, R., Hidayatullah, B. R., Dahlan, E. A., et al. (2018). Design of electromagnetic wave pollutant reducing device using rectenna and circular polarization microstrip antenna[J]. *Advanced Science Letters, 24*(1), 576–580.
28. Li, W., Leung, K. W., & Yang, N. (2018). Omnidirectional dielectric resonator antenna with a planar feed for circular polarization diversity design [J]. *IEEE Transactions on Antennas & Propagation, 66*(3), 1189–1197.
29. Fukusako, T., & Yamauchi, R. (2017). Broadband wave guide antenna using L-shaped probe for wide-angle circular polarization radiation [J]. *Ieice Communications Express, 6*, 53–54.

Lulu Bei was born in Liaoning, Republic of China, in 1981. She received the B.S. degree in Computer Science and Technology from Bohai University, in 2005, and received the M.S. degree in Communication and Information System from Liaoning Technical University, in 2009. She received the Ph.D. degree from China University of Mining and Technology in 2015. In the same year, she joined the Xuzhou Institute of Technology, as a Lecturer. Her current research interests include the Radio Frequency Communication Technology, Microwave components design and Cognitive Radio Techniques

Lu Zhang was born in 1986. He received the Ph.D. degree in Department of Mathematics from University of Macau. He is now a Lecturer in School of Mathematics and Statistics at Xuzhou University of Technology, China. His research interests include numerical algebra and numerical solution of fractional differential equations.

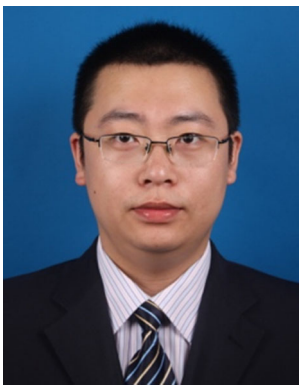

Kai Huang was born in Liaoning, Republic of China, in 1983. He received the B.S. And M.S. degrees in Information Engineering and Communication and Information System from Liaoning Technical University in 2005 and 2009, respectively. He received the Ph.D. degree from China University of Mining and Technology in 2015. In the same year, He joined the Jiangsu XCMG Information Technology CO.,LTD, as a Senior engineer. His present research interests include the Communication and Information Technology, Mine Communication and Information, Wireless Sensor Network and Cognitive Radio Systems